

# Endoscopic endonasal cranial base surgery simulation using an artificial cranial base model created by selective laser sintering

Kenichi Oyama · Leo F. S. Ditzel Filho · Jun Muto · Daniel G. de Souza · Ramazan Gun · Bradley A. Otto · Ricardo L. Carrau · Daniel M. Prevedello

Received: 1 February 2014 / Revised: 22 July 2014 / Accepted: 31 August 2014 / Published online: 17 October 2014  
© Springer-Verlag Berlin Heidelberg 2014

**Abstract** Mastery of the expanded endoscopic endonasal approach (EEA) requires anatomical knowledge and surgical skills; the learning curve for this technique is steep. To a great degree, these skills can be gained by cadaveric dissections; however, ethical, religious, and legal considerations may interfere with this paradigm in different regions of the world. We assessed an artificial cranial base model for the surgical simulation of EEA and compared its usefulness with that of cadaveric specimens. The model is made of both polyamide nylon and glass beads using a selective laser sintering (SLS) technique to reflect CT-DICOM data of the patient's head. It features several artificial cranial base structures such as the dura mater, venous sinuses, cavernous sinuses, internal carotid arteries, and cranial nerves. Under endoscopic view, the model was dissected through the nostrils using a high-speed drill and other endonasal surgical instruments. Anatomical structures around and inside the sphenoid sinus were accurately reconstructed in the model, and several important surgical landmarks, including the medial and lateral optico-carotid recesses

and vidian canals, were observed. The bone was removed with a high-speed drill until it was eggshell thin and the dura mater was preserved, a technique very similar to that applied in patients during endonasal cranial base approaches. The model allowed simulation of almost all sagittal and coronal plane EEA modules. SLS modeling is a useful tool for acquiring the anatomical knowledge and surgical expertise for performing EEA while avoiding the ethical, religious, and infection-related problems inherent with use of cadaveric specimens.

**Keywords** Anatomical model · Cranial base · Endonasal approach · Endoscope

## Introduction

During the past decade, the expanded endoscopic endonasal approaches (EEAs) have been widely used to address ventral cranial base lesions [1–5, 16, 17]. As EEAs represent a radical change in the practice of cranial base surgery, requiring the acquisition of new knowledge and surgical skills must be required [19]. However, the use of cadaveric specimens for this purpose may be hampered by ethical, religious, legal, and biohazard restrictions.

Selective laser sintering (SLS) is a rapid prototyping technology, which employs a laser beam to solidify powder materials such as polycarbonate, nylon, steel, or rubber and builds up models in layers. It has been used to create surgical training models for conventional skull base techniques [11–13, 20, 21].

The 3D cranial base model (Ono & Co. Ltd., Tokyo, Japan) created using the SLS technique has been reported to be a useful tool for the training of surgeons for conventional open cranial base surgery [11, 13]. The model is made of both polyamide nylon and glass beads and features several artificial

**Electronic supplementary material** The online version of this article (doi:10.1007/s10143-014-0580-4) contains supplementary material, which is available to authorized users.

K. Oyama · L. F. S. D. Filho · J. Muto · D. G. de Souza · D. M. Prevedello

Department of Neurological Surgery, The Ohio State University Wexner Medical Center, 410 West 10th Avenue, Columbus, OH 43210, USA

R. Gun · B. A. Otto · R. L. Carrau  
Department of Otolaryngology - Head & Neck Surgery, The Ohio State University Wexner Medical Center, 410 West 10th Avenue, Columbus, OH 43210, USA

K. Oyama (✉)  
Department of Neurological Surgery, Nippon Medical School, 1-1-5 Sendagi, Bunkyo, Tokyo 1130022, Japan  
e-mail: ko-neuro@nms.ac.jp

cranial base structures such as the dura mater, venous sinuses, cavernous sinuses, internal carotid arteries, and cranial nerves. As the model can be created based on the patient anatomy, surgical simulation can be customized and the procedures required to address tumors and individual anatomic variations can be mimicked before the actual operation.

This study assessed this 3D cranial base model for the surgical simulation of EEAs and compared its usefulness with that of cadaveric specimens.

## Materials and methods

For the surgical simulation of EEA, we used the dissectable 3D cranial base model (KEZLEX®A22; Ono & Co. Ltd., Tokyo, Japan), which was created using the SLS technique based on the CT-DICOM data of a patient's head (Fig. 1). For data acquisition, the patient's head was scanned using a multidetector-row computed tomography (Aquilion 64®, Toshiba Medical Systems, Japan). The scanning parameters were slice width, 0.5 mm; helical pitch, 0.641; image production interval, 0.3 mm; X-ray tube voltage, 120 kV; tube current, 300 mA; field of view, 199.68×199.68 mm; pixel size, 0.390×0.390; and scan speed, 0.5 s/rotation [21]. The DICOM data were reconstructed with Mimics® software (Materialise Japan Co., Ltd., Yokohama, Japan) and converted to the standard

triangulation language (STL) file system. The powder material comprised of 30 to 90 % by weight of a synthetic resin (polyamide nylon) and 10 to 70 % by weight of inorganic filler (glass beads) was laser-sintered according to the STL data. The powder of the synthetic resin consisted of spherical particles with an average diameter of 5 to 200 μm. The sintered layers were accumulated with a pitch of 0.1 mm using the SLS method. The 3D cranial base model reproduced all structures needed for the simulation of epidural cranial base approaches, including the anterior clinoid process, the optic canal and strut, the superior orbital fissure (SOF), the foramen rotundum, ovale, and spinosum, and the ethmoid and sphenoid sinus [13]. The periosteal layer of the dura mater was formed from yellow silicone (hydrophilic vinyl polysiloxane impression material, Exafine Hard Type; GC Corporation, Tokyo, Japan) painted onto the inner surface of the orbit to reproduce the periorbita and on the parasellar area of the sphenoid bone to reproduce the medial wall of the cavernous sinus (CS). The dura mater, except for the CS-related areas, was reconstructed with a single layer of the meningeal dura to render it thin, dissectable, and retractable. The meningeal layer was modeled with brown silicone (Exafine Injection Type; GC Corporation). The venous plexuses of the CS were modeled by brushing blue silicone (Exafine Regular Type; GC Corporation, Shanghai, China) onto the yellow silicone of the medial wall. The other venous

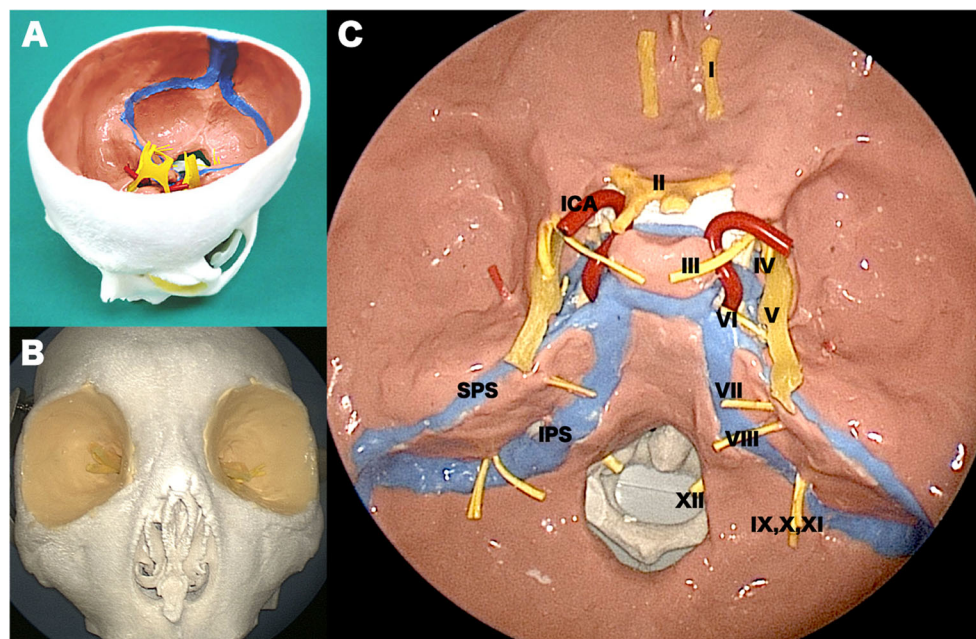


**Fig. 1** The 3D cranial base model created by selective laser sintering. It features several artificial cranial base structures: dura mater, venous sinuses, cavernous sinuses, internal carotid arteries, and cranial nerves. **a** Superior view of the entire model. **b** Frontal view of the model. **c** Intracranial view of the model. All cranial nerves are modeled with either yellow rubber strings or sponges and placed in the corresponding canals. *I*

*olfactory nerve, II optic nerve, III oculomotor nerve, IV trochlear nerve, V trigeminal nerve, VI abducens nerve, VII facial nerve, VIII cochlear nerve, IX glossopharyngeal nerve, X vagal nerve, XI accessory nerve, XII hypoglossal nerve, ICA internal carotid artery, IPS inferior petrosal sinus, MMA middle meningeal artery, SPS superior petrosal sinus*

sinuses were also modeled with blue silicone. The C1 to C6 portions of the internal carotid artery (ICA) were modeled with red vinyl tubes. Cranial nerve (CN) III and IV, and the ophthalmic division (V1) of the trigeminal nerve were modeled with yellow rubber fibers and then placed in the CS and the SOF. The maxillary and mandibular divisions (V2, V3) of the trigeminal nerve were positioned in the foramen rotundum and foramen ovale, respectively. The other cranial nerves were also modeled and inserted in the corresponding foramina. The meningeal layer was modeled with brown silicone (Exafine Injection Type; GC Corporation), and the dura propria (meningeal layer) of the lateral wall in the CS was modeled with brown silicone on the inner reticular layer. Anatomical dissections were performed in the Anatomy Laboratory Toward Visuospatial Surgical Innovations in Otolaryngology and Neurosurgery (ALT-VISION) at The Ohio State University. Visualization and video and photo documentation were with a 4-mm-diameter, 18-cm-long, rod-lens endoscope, featuring 0°, 30°, and 70° lenses. It was connected to a light source via a fiber optic cable and fitted with a 3-chip, high-definition sensor camera coupled to a high-definition monitor and an AIDA digital archiving system (Karl Storz GmbH, Tuttlingen, Germany). The model was fixed with a Mayfield 3-pin head holder. A surgical navigation system (Navigation System II, Stryker Co. Kalamazoo, MI, USA) containing the CT-DICOM data of the model was used to confirm the surgical anatomy as necessary. A high-speed drill (Midas Rex® Legend® EHS Stylus® High-Speed Drill, Medtronic, Inc., Minneapolis, MN, USA) and other single-shaft endoscopic surgical instruments were used for the dissections. The surgical simulations were performed and assessed by three experienced neurosurgeons who compared the differences among the model, the cadaveric specimen, and actual surgery. They discussed and graded the differences in soft tissue dissection, bone dissection, and the acquisition of anatomical knowledge. Grading was from 1 to 5, where 1=the lowest grade (completely different from actual surgery), 3=the middle grade (resembling, but slightly different from, actual surgery; acceptable for training), and 5=the highest grade (same as in actual surgery).

## Results

### Comparison between the skull model and the cadaveric head

The anatomical structures around and inside the sphenoid sinus were accurately reconstructed, and several important surgical landmarks such as the medial and lateral opticocarotid recesses (Fig. 2a), the vidian canals (Fig. 2b), the foramen ovale and rotundum, the jugular

foramen, and the hypoglossal and internal carotid canals were clearly visible during dissection [6, 8, 18]. Since the model is bright white, the endoscopic view was clearer than that of the cadaveric specimens. Almost all of the skull base was covered by artificial dura mater. Not covered were the pituitary fossa and surrounding structures, including a part of the CSs and the internal carotid canals. The bone could be removed with a high-speed drill until it was eggshell thin, preserving the dura mater. This emulated the surgical technique used during endonasal cranial base approaches in patients.

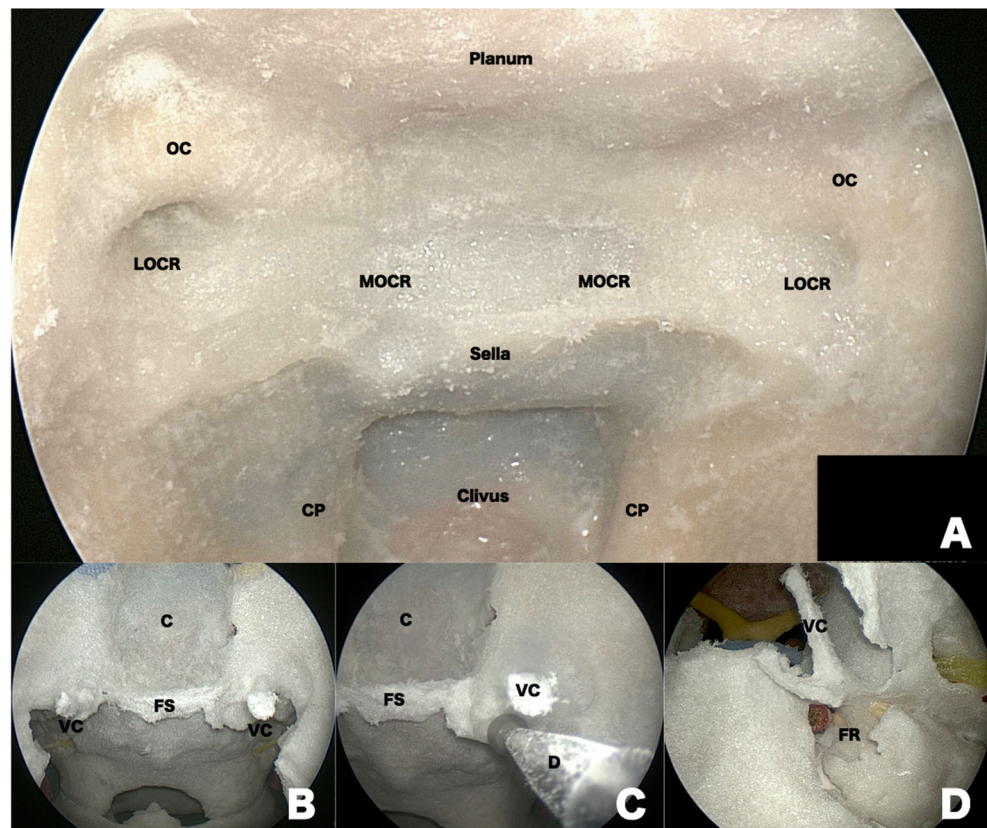
As shown in Table 1, there were differences between the skull model and cadaveric head specimens with respect to the surgical simulation of EEAs. As the model lacks several soft tissue structures, including the nasopharyngeal mucosa, fascia, ligaments, and muscle, the complexity of soft tissue dissection was not encountered. The artificial skull bone, made of a combination of polymer and glass beads, was slightly harder than human bone. Drilling turned it into powder that was easily removed by suctioning or irrigating with water, in a manner similar to the technique used in cadaveric specimens. At times, the dust created during drilling was slightly sticky and adhered to the surgical instruments. The powder not laser-hardened remained in the paranasal sinuses and the cavity of cancellous bone. Setting up the navigation system was easier with the model than with cadaveric specimens because it could be accomplished by using preexisting model CT-DICOM data; confirming the anatomical bone landmarks with the frameless stereotactic navigation was accurate. As, unlike with cadaveric specimens, there is no risk of pathogenic infection, the model can be used for practice of anatomical dissections outside the anatomical lab.

### Surgical simulation in the sagittal plane module: anterior skull base to C2

#### Transsellar approach

The procedure started with the removal of the middle turbinate. A posterior septectomy created a binarial corridor to allow increased freedom of movement. The middle turbinate of the left naris was lateralized. After wide bilateral sphenoidotomies, several important surgical landmarks, including the medial and lateral optico-carotid recesses and carotid protuberances, could be clearly observed (Fig. 2a). The sellar floor was opened using a high-speed microdrill and a Kerrison rongeur (Fig. 3a). As the model lacked artificial dura mater around the pituitary gland in the sella turcica, opening its floor revealed an inferior intercavernous sinus, an empty sella, and dorsum sellae (Fig. 3b).

**Fig. 2** Endonasal view with 0° endoscope. **a** The anatomical landmarks within the sphenoid sinus are accurately reconstructed. **b** The vidian canal is located at the floor of the sphenoid sinus. **c** The vidian canal is dissected toward the foramen lacerum and the anterior genu of the ICA. **d** The anatomical relationship between the vidian canal and foramen lacerum as seen from below. *C* clivus, *CP* carotid protuberance, *D* high-speed drill, *FL* foramen lacerum, *FS* floor of sphenoid sinus, *LOCR* lateral optico-carotid recess, *MOCR* medial optico-carotid recess, *OC* optic canal, *VC* vidian canal



#### Transplanum/transuberculum approach (Video 1)

To perform wide, bilateral posterior ethmoidectomies, the ethmoid septations were drilled flush with the anterior cranial base and reduced laterally to the level of the lamina papyracea. The tuberculum sellae and planum sphenoidale were drilled down. Drilling the bone to eggshell thickness and elevating it from the underlying tissue preserved the dura as in actual surgery and in cadaveric specimens (Fig. 3c).

**Table 1** Comparison between the artificial 3D skull model and a cadaver head for the simulation of endoscopic endonasal skull base surgery

	Skull model grade	Cadaver head grade
Simulation of soft tissue dissection	1	4
Simulation of bone dissection	3	4
Acquisition of anatomical knowledge	3	5

Grading was from 1 to 5 where 1 is the lowest grade (completely different from actual surgery), 3 is the middle grade (resembling but slightly different from actual surgery and acceptable for training), and 5 is the highest grade (same as in actual surgery)

#### Transcribriform approach

After bilateral total sphenoid-ethmoidectomies, the bony grooves of the anterior and posterior ethmoidal arteries were identified (Fig. 3d). After the bony component of the anterior skull base was drilled down and a Draf III procedure was performed (Fig. 3e), the crista galli was dissected off the dura mater in a manner similar to the procedure used in vivo and in cadaveric specimens (Fig. 3f).

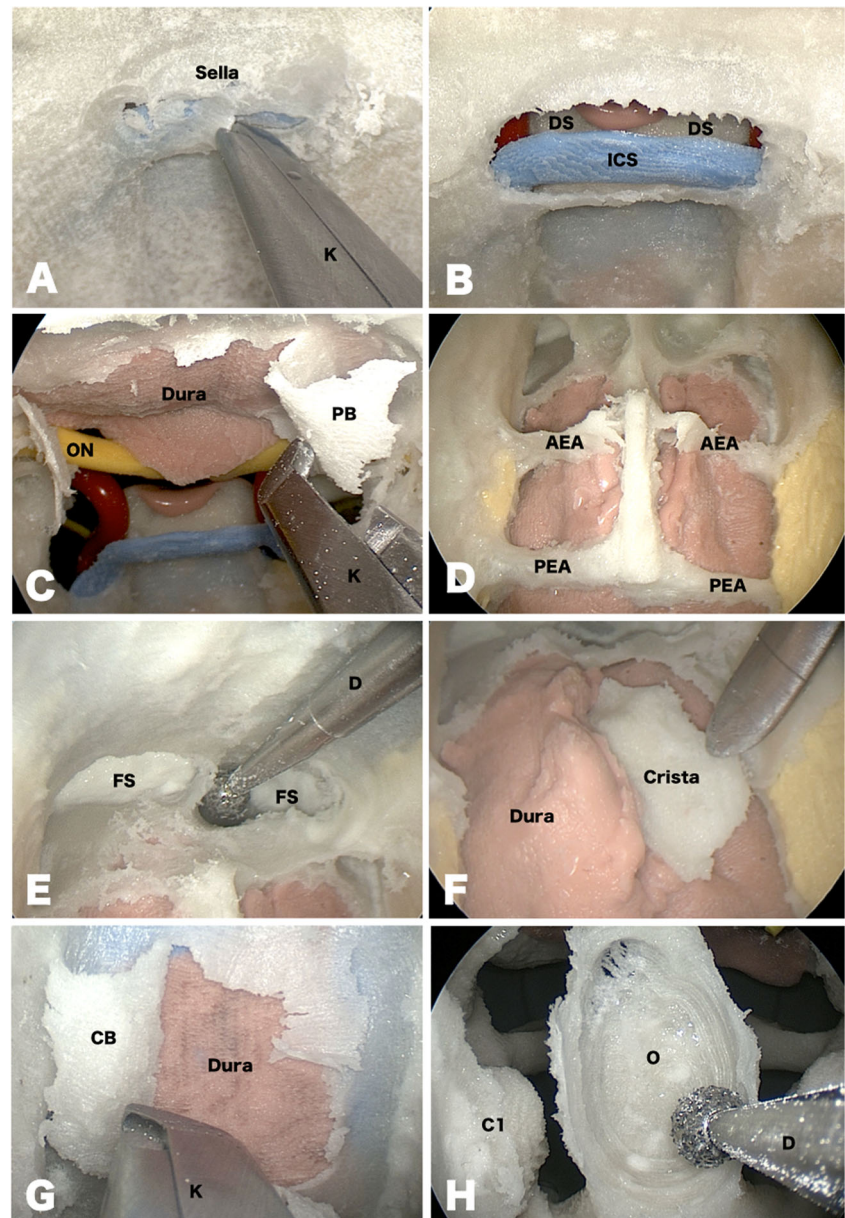
#### Transclival approach

The floor of the sphenoid sinus was drilled down, following the vidian canals toward both lacerum foramina, until flush with the clivus. Next, the clival bone itself was drilled. The dura mater was once again preserved as in procedures performed in vivo and in cadaveric specimens (Fig. 3g).

#### Transodontoid approach

After removing the anterior arch of C1, the dens was drilled centrally, leaving a shell of cortical bone (Fig. 3h). The remaining bone was removed with a Kerrison rongeur. Due to the absence in the model of the nasopharyngeal mucosa, basipharyngeal fascia, and ligaments tethering the dens, we

**Fig. 3** Surgical simulation in the sagittal plane module. **a, b** Transsellar approach. As the model did not feature the artificial dura matter and pituitary gland in the sella turcica, the inferior intercavernous sinus, an empty sella, and dorsum sellae were identified after opening the sellar floor. **c** Transplanum/transuberulum approach. The bone of the planum sphenoidale is drilled to eggshell thickness and peeled off the dura. **d, e, f** Transcribriform approach. The bony grooves of the anterior and posterior ethmoidal arteries were identified (**d**). After drilling off the bone of the anterior skull base and performing a Draf III procedure (**e**), the crista galli can be dissected and removed from the dura mater (**f**). **g** Transclival approach. The clival bone between both carotid protuberances is drilled to an eggshell thickness and peeled off the dura. **h** Transodontoid approach. After partial removal of the arch of C1, the dens is cored out. *AEA* anterior ethmoidal artery, *C1* arch of the first cervical vertebra (partially removed), *CB* clival bone, *Crista* crista galli, *DS* dorsum sellae, *FS* frontal sinus, *ICS* intercavernous sinus, *ON* optic nerve, *PB* planum bone, *PEA* posterior ethmoidal artery, *O* odontoid process of the second cervical vertebra



could not assess the complexity involved in dissecting those structures. In addition, as the model did not feature the soft palate or the pharynx, dissection of the odontoid with surgical instruments was easier than is the case in actual surgery and in cadaveric specimens.

### Surgical simulation in the coronal plane module: cavernous sinus to infratemporal fossa

#### Cavernous sinus approach

After performing a wide sphenoidotomy, a bony window in front of the cavernous sinus was opened, using a high-speed

microdrill and a Kerrison rongeur. As there was no artificial dura mater in the anterior aspect of the CS, the artificial ICA and the CN III and IV, and trigeminal nerves were immediately visible (Fig. 4a).

#### Transorbital approach

The lamina papyracea was drilled until only a layer of paper-thin bone layer remained over the periorbita; it was then removed with a Cottle elevator to complete the decompression of the medial orbital wall (Fig. 4b). As the model does not feature an artificial eyeball inside the orbit, the periorbita was pushed from the medial aspect of the orbit to confirm the extent of the decompression.

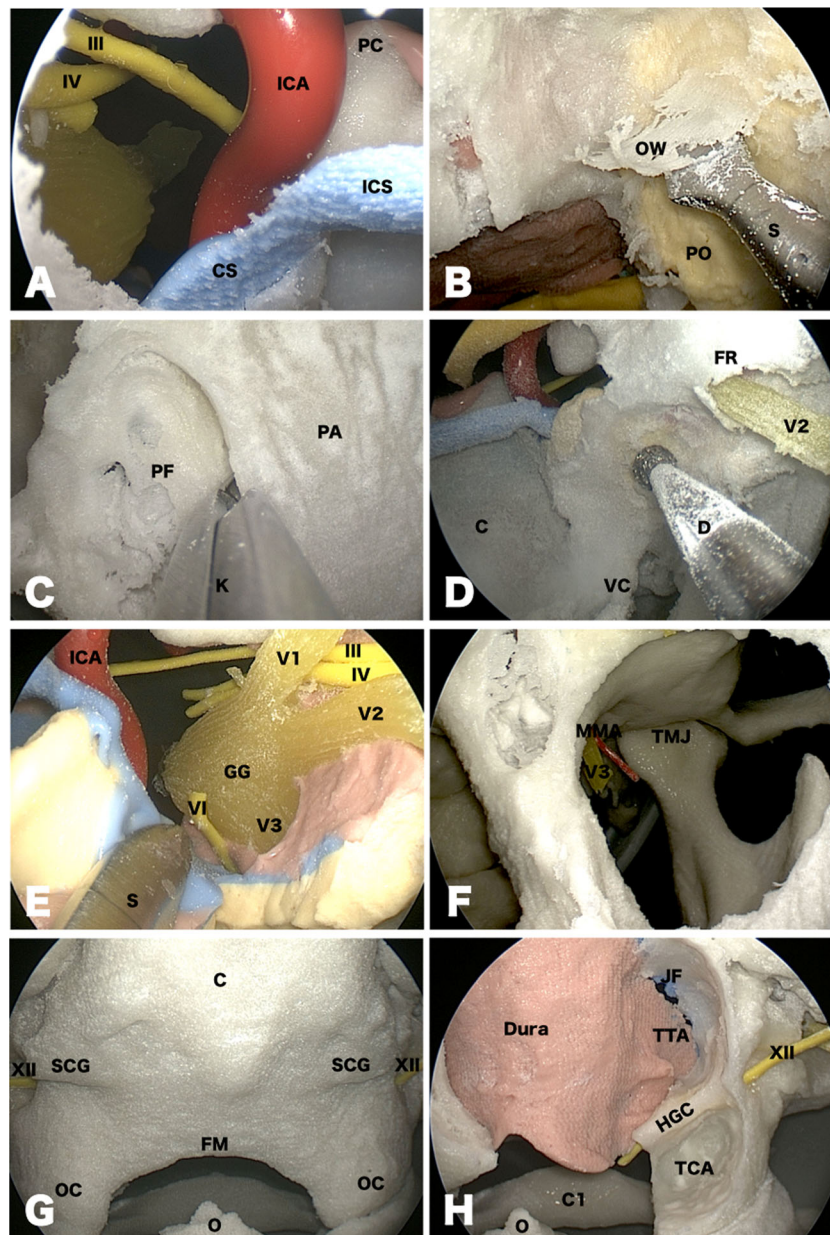


**Fig. 4** Surgical simulation in the coronal plane module. **a** Cavernous sinus approach. After removing the bone in front of the right cavernous sinus, the artificial internal carotid artery and cranial nerves could be seen. **b** Transorbital approach. The lamina papyracea is drilled to paper-thinness and removed with a Kerrison rongeur to complete the unroofing of the medial orbital wall. **c, d, e** Meckel's cave approach/suprapetrous approach. The bone between V2 and the vidian canal was removed with a high-speed drill and rongeur (**c, d**) to expose the periosteal dural layer overlying the anterior surface of Meckel's cave. After opening the periosteal dura, the trigeminal and other cranial nerves can be visualized (**e**). **f** Infratemporal fossa approach. As no soft tissue was present within the infratemporal fossa, V3, the middle meningeal artery, and the temporomandibular joint could be easily observed. **g, h** Far medial approach. In the lower clival region, the supracondylar groove could be clearly

identified (**g**). A transcondylar/transjugular tubercle approach was performed (**h**). III oculomotor nerve, IV trochlear nerve, V trigeminal nerve, VI abducens nerve (partially represented), XII hypoglossal nerve, C1 arch of the first cervical vertebra, C clivus, CS cavernous sinus (partially represented), FR foramen rotundum, FM foramen magnum, GG gasserian ganglion, HGC hypoglossal canal, ICA internal carotid artery, ICS intercavernous sinus, JF jugular foramen, MMA middle meningeal artery, O tip of the odontoid process, OC occipital condyle, OW orbit wall, PA posterior wall of the antrum, PC posterior clinoid, PF pterygopalatine fossa, PO periorbita, S spatula, SCG supracondylar groove, TCA transcondylar approach, TMJ temporomandibular joint, TTA transjugular tubercle approach, V2 maxillary division of the trigeminal nerve, VC vidian canal, V1 ophthalmic division of the trigeminal nerve, V3 mandibular division of the trigeminal nerve

### Meckel's cave approach/ supratentorial approach (Video 2)

A wide nasomaxillary window was opened and the posterior wall of the antrum was removed with a Kerrison rongeur and a high-speed drill. This exposed the pterygopalatine fossa (Fig. 4c). Due to the absence of fat tissue or vascular structures inside the pterygopalatine fossa, the V2 and the foramen rotundum were easily identifiable. The bone between V2 and the vidian canal was removed with a high-speed drill and a rongeur to expose the periosteal dural layer overlying the anterior surface of Meckel's cave (Fig. 4d). After opening the periosteal dura, the gasserian ganglion and all trigeminal branches (ophthalmic-V1, maxillary-V2, mandibular-V3) as well as other the CN III, IV, and VI were visualized (Fig. 4e) in the position they are found in actual surgery or cadaveric dissection.

### Infratemporal fossa approach

For the transpterygoid infratemporal fossa dissection, the antrostomy was extended anteriorly with a backbiter and the base of the pterygoid plates was exposed. Since the lateral pterygoid and temporalis muscle were absent in the infratemporal fossa, V3, the middle meningeal artery, and the temporomandibular joint were observed in the position they are found in actual surgery or cadaveric dissection (Fig. 4f).

### Far medial approach (Video 3)

In the lower clival region, the supracondylar groove indicating the position of the hypoglossal canal [10] could be clearly identified (Fig. 4g); transcondylar and transjugular tubercle approaches could be performed (Fig. 4h). During drilling, it was possible to differentiate between the cancellous bone of the condyle and the jugular tubercle and the compact bone of the hypoglossal canal; this facilitated its preservation. When drilling the model's cancellous bone, the soft consistency characteristic of this type of bone could be felt and unhardened powder material within air cells was encountered. On the other hand, when drilling over the compact bone of the hypoglossal canal, its consistency was hard; this facilitated its preservation as in actual surgery.

## Discussion

In skull base surgery, endoscopic approaches have become an important alternative to traditional transcranial approaches. Consequently, neurosurgeons must acquire new surgical skills. To acquire these, surgeons attend courses and hands-on laboratory sessions, observe and assist experienced

surgeons, and perform surgery under the supervision of experienced surgeons until they are able to operate independently [19].

Cadaveric dissection is an important step in the acquisition of anatomical knowledge and surgical skills for EEA. However, ethical, religious, legal, and biohazard concerns may preclude the performance of cadaveric dissections.

Artificial cranial base models created by SLS avoid these problems and have proven to be valuable for the training of surgeons in conventional open skull base approaches [11–13, 20, 21]. Our study demonstrates the usefulness of the 3D dissectable cranial base models created by SLS for training in EEA.

There was a difference with respect to bone between the cadaveric and the present SLS model. Drilling the model bone feels somewhat different from drilling human bone. The polymer and glass bead combination is slightly harder than the human bone, and the bone dust created during drilling can be slightly sticky and adhere to surgical instruments. Artificial material that resembles bone more closely and new technologies to exclude the presence of powder material in bony cavities are needed. Also, as the model lacks several soft tissue structures, one of the most important aspects of endonasal cranial base surgery is not experienced. Consequently, the 3D model must be further improved for the realistic simulation of endonasal cranial base approaches.

Several methods that use alternatives to cadaveric specimens for EEA training have been reported. They include the model constructed with gelatin [9], the plastic surgical training model that uses eggs [14, 15], and personal webcam trainers [7]. Those training methods, including this 3D cranial base model we examined, eliminate religious and/or legal concerns related to the use of cadaveric specimens and the issue of infection by pathogens or contamination by human-tissue-preserving chemicals. Among those training methods, the 3D model is unique because trainees can simulate the bone drilling, feeling the difference between the compact and the cancellous bone. In addition, the 3D model facilitates a pre-operative “virtually real” simulation of the operative procedure as it is reconstructed based on patient CT data (Table 2).

**Table 2** Advantages of the artificial 3D skull model for the simulation of endoscopic endonasal skull base surgery simulation

	Skull model	Cadaver head
Navigation usage	⊙	○
Reconstruction with patient's data	⊙	×
Avoidance of religious violation	⊙	△
Avoidance of legal violation	⊙	△
Avoidance of pathogenic infection	⊙	△

⊙ = very good, ○ = good, △ = not good, × = poor

The model can be handled and scrutinized in the operating room, or on the surgeon's desk, and it can be dissected at academic meetings to demonstrate techniques and detailed points of anatomy [21]. Unlike cadaver heads, its shelf life is not limited and it remains available for later study. Finally, it can be employed as a model to evaluate the skills of residents and fellows in training. Based on these considerations, we suggest that the 3D model is of heuristic value, especially for the training of surgeons learning to perform EEA.

## Conclusion

The model created by SLS is a useful tool for the acquisition of anatomical knowledge and the surgical simulation of endoscopic endonasal cranial base surgery. It can be used for surgical training and simulations and avoids ethical, legal, and infection-related concerns. It is also suitable for educational purposes. Additional improvements in the 3D model, particularly with respect to soft tissue modeling, will enhance the quality of surgical simulations of endonasal cranial base surgery.

**Disclosures** This study was performed with a grant support from The Japanese Foundation for Research and Promotion of Endoscopy; it was performed at the ALT-VISION lab at The Ohio State University. The ALT-VISION lab receives unrestricted educational supports from the following companies: Carl Zeiss Microscopy, Intuitive Surgical Corp., KLS Martin Corp., Karl Storz Endoscopy, Leica Microscopy, Medtronic Corp., Stryker Corp., and Vycor Medical. The authors have no personal financial or institutional interest in any of the drugs, materials, and devices described in this article.

## References

- Cappabianca P, Cavallo LM, de Divitiis E (2004) Endoscopic endonasal transsphenoidal surgery. *Neurosurgery* 55:933–941
- Carrau RL, Jho HD, Ko Y (1996) Transnasal-transsphenoidal endoscopic surgery of the pituitary gland. *Laryngoscope* 106:914–918
- Jho HD, Carrau RL (1997) Endoscopic endonasal transsphenoidal surgery: experience with 50 patients. *J Neurosurg* 87:44–51
- Kassam A, Snyderman CH, Mintz A, Gardner P, Carrau RL (2005) Expanded endonasal approach: the rostrocaudal axis. Part I. Crista galli to the sella turcica. *Neurosurg Focus* 19:E3
- Kassam A, Snyderman CH, Mintz A, Gardner P, Carrau RL (2005) Expanded endonasal approach: the rostrocaudal axis. Part II. Posterior clinoids to the foramen magnum. *Neurosurg Focus* 19:E4
- Kassam AB, Vescan AD, Carrau RL, Prevedello DM, Gardner P, Mintz AH, Snyderman CH, Rhoton AL Jr (2008) Expanded endonasal approach: vidian canal as a landmark to the petrous internal carotid artery. *J Neurosurg* 108:177–183
- Hirayama R, Fujimoto Y, Umegaki M, Kagawa N, Kinoshita M, Hashimoto N, Yoshimine T (2013) Training to acquire psychomotor skills for endoscopic endonasal surgery using a personal webcam trainer. *J Neurosurg* 118(5):1120–1126
- Labib AM, Prevedello DM, Fernandez-Miranda JC, Sivakanthan S, Benet A, Morera V, Carrau R, Kassam A (2013) The medial

- opticocarotid recess: an anatomic study of an endoscopic “key landmark” for the ventral cranial base. *Neurosurgery* 72:66–76
- Malekzadeh S, Pfisterer MJ, Wilson B, Na H, Steehler MK (2011) A novel low-cost sinus surgery task trainer. *Otolaryngol Head Neck Surg* 145(4):530–533
- Morera VA, Fernandez-Miranda JC, Prevedello DM, Madhok R, Barges-Coll J, Gardner P, Carrau R, Snyderman CH, Rhoton AL, Kassam AB (2010) “Far-medial” expanded endonasal approach to the inferior third of the clivus. *Neurosurgery* 66:211–220
- Mori K, Yamamoto T, Oyama K, Ueno H, Nakao Y, Honma K (2008) Modified three-dimensional skull base model with artificial dura mater, cranial nerves, and venous sinuses for training in skull base surgery: technical note. *Neurol Med Chir (Tokyo)* 48(12):582–588
- Mori K, Yamamoto T, Oyama K, Nakao Y (2009) Modification of three-dimensional prototype temporal bone model for training in skull-base surgery. *Neurosurg Rev* 32(2):233–239
- Mori K, Yamamoto T, Nakao Y, Esaki T (2010) Development of artificial cranial base model with soft tissues for practical education. *Neurosurgery* 66:339–341
- Ogino-Nishimura E, Nakagawa T, Sakamoto T, Ito J (2012) An endoscopic endonasal surgery training model using quail eggs. *Laryngoscope* 10:2154–2157
- Okuda T, Kataoka K, Kato A (2010) Training in endoscopic endonasal transsphenoidal surgery using a skull model and eggs. *Acta Neurochir (Wien)* 152(10):1801–1804
- Oyama K, Ikezono T, Tahara S, Shindo S, Kitamura T, Teramoto A (2007) Petrous apex cholesterol granuloma treated via the endoscopic transsphenoidal approach. *Acta Neurochir (Wien)* 149(3):299–302
- Prevedello DM, Doglietto F, Jane JA Jr, Jagannathan J, Han J, Laws ER Jr (2007) History of endoscopic skull base surgery: its evolution and current reality. *J Neurosurg* 107:206–213
- Rhoton AL Jr (2002) The sellar region. *Neurosurgery* 51:335–374
- Snyderman C, Kassam A, Carrau R, Mintz A, Gardner P, Prevedello DM (2007) Acquisition of surgical skills for endonasal skull base surgery: a training program. *Laryngoscope* 117:699–705
- Suzuki M, Ogawa Y, Kawano A, Hagiwara A, Yamaguchi H, Ono H (2004) Rapid prototyping of temporal bone for surgical training and medical education. *Acta Otolaryngol* 124(4):400–402
- Wanibuchi M, Ohtaki M, Fukushima T, Friedman AH, Houkin K (2010) Skull base training and education using an artificial skull model created by selective laser sintering. *Acta Neurochir (Wien)* 152:1055–1060

## Comments

Domenico Solari, Luigi Maria Cavallo, Naples, Italy

In this interesting article, coming from an experienced group in the field of endoscopic skull base surgery, the importance of an integrated know-how of anatomical knowledge and surgical attitude has been highlighted. Moreover, authors added an extra value with this innovative method that gives the opportunity to perform an excellent lab rehearsal. In these regards, the authors should be praised for having applied this laser DICOM-based sintering technique that can help in acquiring spatial relationships and defining properly the surgical possibilities of the approach as run in the lab training. They shed light on the need for technological progress and surgical refinements but, at same time, confirmed the need for anatomic knowledge as well as surgical hand and mind skills, regardless of the tools or the technique. A thorough anatomical knowledge as well as a comprehensive, fully computer-integrated, preoperative study is mandatory to create a strictly decision making process. This innovative tool seems to fit this requirement; nevertheless, it should be well evaluated its cost-effectiveness also according to a proper case selection.